

Original Article

Applying deep learning-based regional feature recognition from macro-scale image to assist energy saving and emission reduction in industrial energy systems

Siliang Chen¹, Xu Zhu¹, Kang Chen, Zexu Liu, Pengcheng Li, Xinbin Liang, Xinqiao Jin, Zhimin Du^{*}

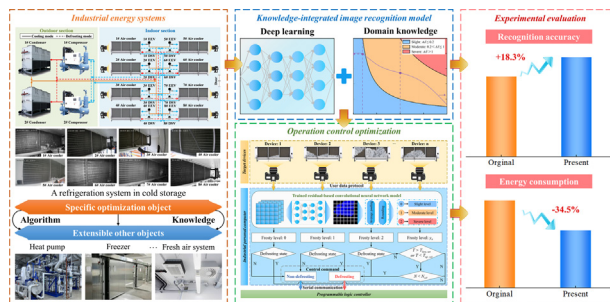
School of Mechanical Engineering, Shanghai Jiao Tong University, Shanghai 200240, China

HIGHLIGHTS

- A novel energy knowledge-integrated image recognition technology was applied to assist energy savings.
- Non-physical image information was combined with specific energy domain knowledge for the first time.
- The proposed image recognition model enables both high recognition accuracy and strong generalization ability.
- The energy consumption reduces by 34.5% through adopting image recognition-based control optimization method.
- The proposed control optimization method can be easily extended to general energy systems.

GRAPHICAL ABSTRACT

By integrating advanced deep learning and specific energy domain knowledge, Chen et al. develop a novel deep learning-based image recognition to assist energy saving and emission reduction for industrial energy systems, which greatly increases the recognition accuracy by 18.3% and decreases the energy consumption by 34.5%.



ARTICLE INFO

Article history:

Received 13 February 2022

Revised 6 June 2022

Accepted 16 July 2022

Available online xxxx

Keywords:

Deep learning
Knowledge-integrated image recognition
Industrial energy system
Operation control optimization
Experimental evaluation

ABSTRACT

Introduction: Image recognition technology has immense potential to be applied in industrial energy systems for energy conservation. However, the low recognition accuracy and generalization ability under actual operation conditions limit its commercial application.

Objectives: To improve the recognition accuracy and generalization ability, a novel image recognition method integrating deep learning and domain knowledge was applied to assist energy saving and emission reduction for industrial energy systems.

Methods: As a typical industrial scenario, the defrosting control in the refrigeration system was selected as the specific optimization object. By combining deep learning algorithm with domain knowledge, a residual-based convolutional neural network model (RCNN) was proposed specifically for frosty state recognition, which features the residual input and average pooling output. Based on the real-time recognition of frosty levels, a defrosting control optimization method was proposed to initiate and terminate the defrosting operation on demand.

Results: By combining the advanced image recognition technique with specific energy domain knowledge, the proposed RCNN enables both high recognition accuracy and strong generalization ability. The recognition accuracy of RCNN reached 95.06% for the trained objects and 93.67% for non-trained objects while that of only 75.86% for the conventional CNN. By adopting the presented system optimization method assisted by RCNN, the defrosting frequency, accumulated time and energy consumption were

Peer review under responsibility of Cairo University.

* Corresponding author.

E-mail address: duzhimin@sjtu.edu.cn (Z. Du).

¹ These authors contributed equally to this work.

53.8%, 57.02% and 34.5% less than the original control method. Furthermore, the environmental and cost analysis illustrated that the annual reduction in CO₂ emissions is 2145.21 to 3412.84 kg and the payback time was less than 2.5 years which was far below the service life.

Conclusion: The technical feasibility and significant energy-saving benefits of deep learning-based image recognition method were demonstrated through the field experiment. Our study shows the great application potential of image recognition technology and promotes carbon neutrality in industrial energy systems.

© 2022 The Authors. Published by Elsevier B.V. on behalf of Cairo University This is an open access article under the CC BY-NC-ND license (<http://creativecommons.org/licenses/by-nc-nd/4.0/>).

Introduction

With the rising demand for producing electricity, the utilization of fossil energy has caused severe environmental pollution and a large amount of CO₂ emissions [1]. In order to protect the ecological security of the earth, the Paris Agreement proposed the goal of holding the increase of global temperature not to exceed 2 °C and striving to control it below 1.5 °C [2,3]. Moreover, China has solemnly promised CO₂ emissions will peak by 2030 and strive to achieve carbon neutrality by 2060 at the 75th United Nations General Assembly [4]. Currently, about 37% of the total global energy is consumed in the industrial sector like process heating, boiler operations and refrigeration systems [5,6]. Therefore, industrial energy systems are strongly encouraged to develop advanced technologies for reducing energy consumption and CO₂ emissions.

The energy saving and emissions reduction technologies in the industrial field is the multi-objective optimization for energy efficiency, economic benefits and pollutants emissions, which can be roughly divided into three types: model-based, knowledge-based and data-driven methods [7,8]. With the rapid development of artificial intelligence (AI) algorithms and big data analyses [9], the data-driven method has received increasing attention in industry and academia [10], especially in the field of energy-saving technologies. Recently, significant progress has been made in various data-driven methods to implement industrial energy conservation measures. Advanced data-driven methods like deep learning [11], intelligent optimization [12] and data mining [13] have been proved to effectively reduce the energy consumption and carbon emissions in every industrial link, and display excellent prospects for practical application in industrial energy systems.

The refrigeration system plays a crucial role in ensuring the operating environment and staff comfort in the industry [14]. About 15% of the world's energy consumption and 10% of greenhouse gas emissions are dominated by the refrigeration system [15]. However, Frost formation is the most detrimental and essential problem that happens on the heat exchangers in the refrigeration system, which severely jeopardizes the operating efficiency and stability [16]. In order to avoid unnecessary or belated defrosting cycles, accurate measurement of the frosty state is considered the key and foundation to establish a well-functioning defrosting control strategy. Although numerous measurement methods [17–22] have been presented in recent years, the high initial cost, restricted detection region and strict installation requirements restrict their further development and application. For reasons of low cost and easy operation, researchers and engineers pay much attention to the function of image processing technology in frosty state detection [23]. Based on grayscale conversion and threshold division, the frosting zone and non-frosting zone in the image are determined directly, and the frosty level can be quantitatively analyzed [24–26]. It has been demonstrated that image recognition technology has immense potential to be applied in industrial energy systems for control optimization and energy savings.

Although significant efforts have been made in developing image recognition-based control optimization technology, there are still some limitations in the existing literature. On the one hand,

almost all methods are short of generalization ability. With respect to different shooting angles and illumination levels, the establishment of image recognition model depends on time-consuming experiments and labor-intensive image labeling workload, which lead to considerable cost and labor consumption. On the other hand, the recognition accuracy of current approaches might deteriorate in practical application. The selections of frosty feature such as grayscale and color are hard to reflect the complex variation of recognition object in different external factors and often overlooks the importance of domain knowledge, which might lead to the low recognition accuracy under actual operation conditions. Above demerits are the common problems for image recognition-based energy-efficient technology, which severely compromise its commercial applications in industrial energy systems. In this study, we aim to improving the recognition accuracy and generalization ability of image recognition model by integrating the specific energy domain knowledge and advanced deep learning algorithm, and optimizing the control strategy in industrial energy systems based on the well-designed image recognition model.

Therefore, a novel deep learning-based image recognition method was presented to assist energy saving and emission reduction for industrial energy systems in this paper. As a typical industrial energy consumption scenario, we selected the defrosting control in the refrigeration system as the specific optimization object. By integrating the domain knowledge and advanced image recognition technique, a residual-based convolutional neural network (RCNN) model was proposed specifically for frosty state recognition, which is characterized by the residual input and average pooling output. Based on the trained RCNN model, a defrosting control optimization method was proposed to initiate and terminate the defrosting operation on demand according to the real-time frosty level. The field experiment was conducted to evaluate the application feasibility and energy-saving performance of the proposed method. Furthermore, the environmental and cost analysis was carried out to assess the environmental benefit and commercial value. The above study is expected to promote the practical application of deep learning-based energy-efficient technology in industrial energy systems.

Materials and methods

Smart AI technology is developing rapidly and has the potential to be applied in various fields and assisted in various scenarios. As a typical industrial scenario, the refrigeration system in the cold storage can provide an appropriate temperature and humidity environment to maintain the quality and safety of food, flowers and drugs. The operation control strategy directly impacts energy consumption and carbon emissions of the refrigeration system, which has become an increasingly important research topic, especially in developing countries. Consequently, we selected the refrigeration system in the cold storage as the specific research object, and apply deep learning-based image recognition technology for its operation control optimization. The schematic overview of the proposed defrosting control optimization method is shown in Fig. 1, which

is composed of four stages: field experiment, image labeling and transformation, deep learning-based image recognition model and operation optimization. The field experiment is carried out to obtain the datasets used for training and verifying the technical feasibility of the proposed method. The image preprocessing stage aims to improving the quality of input for training the image recognition model, including image labeling and image transformation. The presented deep learning-based RCNN model is utilized for the feature extraction and frosty levels recognition of captured images with high generalization ability. Based on the real-time recognition for frosty levels, the defrosting control optimization method is further proposed to initiate and terminate the defrosting operation on demand. According to the current frosty level and pre-determined control strategy, the industrial personal computer (IPC) sends control commands to the programmable logic controller (PLC) to finally accomplish demand-based defrosting control.

Datasets from field experiments of typical industrial scenario

Frost images and operational data of the refrigeration system are the basis for developing the AI models. To obtain the frosty images and operating parameters datasets for the training and verification of proposed method, the field experiment was conducted in an industrial energy system on site, the refrigeration system of cold storage in Nanjing City, Jiangsu Province. The refrigeration system is composed of two screw compressors, two evaporative condensers, eight air coolers, eight electronic expansion valves (EEV) and eight defrosting solenoid valves (DSV). The schematic diagram of the experimental system is shown in Fig. 2a. The total cooled floor area of the experimental field is 1800 m². Under cooling mode, the gas transmission capacity of compressors is controlled by the slide valve to adjust the refrigerating capacity according to the operating conditions. Under the defrosting mode, the refrigerant discharged from the compressors passes through the defrosting solenoid valve to melt the frost in the air coolers and then flows back into the compressors. The experimental system's detailed description and equipment configuration are given in Note. S1 (online).

In order to validate the technical feasibility of the proposed defrosting control optimization method in practical application, the field experiment lasted for two months. In the former month, the refrigeration system maintains the original time-based defrosting mode, i.e., defrosting the air cooler for 30 min after operating per 12 h. During this period, the frosty states on the surfaces of eight air coolers were photographed by surveillance cameras per 5 min. The shooting angle and illuminance intensity of each air cooler is shown in Fig. 2b. Due to the different on-site installation conditions of surveillance cameras, the shooting angles and illuminance intensities are distinct among all air coolers. For the whole captured images, part of the air coolers' images was divided into the training and testing datasets, while the images of other air coolers were entirely taken as the testing dataset. The training and testing datasets were used to train the image recognition model, and inspect its recognition accuracy and generalization performance. In the latter month, the trained image recognition model was utilized in the experimental system for the real-time frosty state recognition, and the optimized defrosting control strategy was adopted to implement the defrosting cycles. The defrosting frequency, accumulated time and energy consumption of each air cooler were compared with that in the former month to demonstrate the technical superiority of the proposed method.

Image labeling and transformation method towards industrial energy systems

Original images obtained from the experimental system need to be processed and normalized before the model development

according to different learning tasks. Differing from the conventional image labeling and transformation approaches in image recognition, we propose a domain knowledge-assisted image preprocessing method by fusing physical mechanisms into image processing process to improve recognition accuracy and generalization ability. For the process of image labeling, the key priority is to determine the categorization criteria of frosty levels. On account of frosting inhomogeneity and its impact on heat transfer capacity, the proportion of frost area (A) and frost thickness (δ) are taken as the classification indicators to divide the frosty states into three levels: slight, moderate and severe frosting. The frosty states of $A\delta \leq 0.2$, $0.2 < A\delta \leq 1$ and $A\delta \geq 1$ are classified as the slight, moderate and severe levels respectively. The detailed classification criteria and basis are illustrated in Note. S2 (online)

The image transformation process includes four steps: residual image acquisition, image augmentation processing, normalization and mapping to RGB color space. Due to the installation and operating constraints of surveillance cameras, the captured images appear in different shooting angles and illuminance intensities for different devices and even include irrelevant background objects, which would shapely reduce the recognition performance of the deep learning model for untrained devices. In order to enhance the generalization ability, the frosty images are subtracted by selected non-frost images from corresponding devices to obtain residual images in which only frosty states vary. Subsequently, the residual images are processed by image augmentation techniques to further improve the generalization performance. The detailed procedures and parameters of the image augmentation process are shown in Note. S3 (online). After the above treatments, the images are normalized and mapped to RGB color space, and then outputted to the image recognition model.

Deep learning-based image recognition model

Based on the preprocessed images obtained from image labeling and transformation methods, we present a novel CNN deep learning model specifically designed for frosty level recognition, named RCNN, which features the residual input and average pooling output. The network architecture of the proposed RCNN model is shown in Fig. 1. The residual image processed by image transformation is provided as the input of the model. For extracting the complicated and in-depth frosty features, the state-of-art backbone like EfficientNet [27], SENet [28] or ResNeXt [29] is utilized in network building to boost the features learning from multifarious frosty images. To further obtain the features for frosty levels classification, the extracted features are normalized, reshaped and fully connected to form the frosty score map. Considering that the frosty level is described as the average frosty state of the whole image, the frosty score map is processed by average pooling to get the frosty score, and the rounded frosty score is regarded as the frosty level of input image. The residual images and average frosty score are respectively used as the model input and output, which helps to eliminate the effects derived from the device shape, the shooting angle, the irrelevant background and the location of frosty zones, and significantly improve the recognition accuracy and generalization performance of the proposed RCNN model. Based on the stochastic gradient descent method, the loss between the real labels and the recognized results is propagated back, and the parameters of the RCNN model are continuously adjusted until reduced to an acceptable range, thus eventually accomplishing the model training process. The detailed training process of RCNN model can be seen in Note. S4 (online).

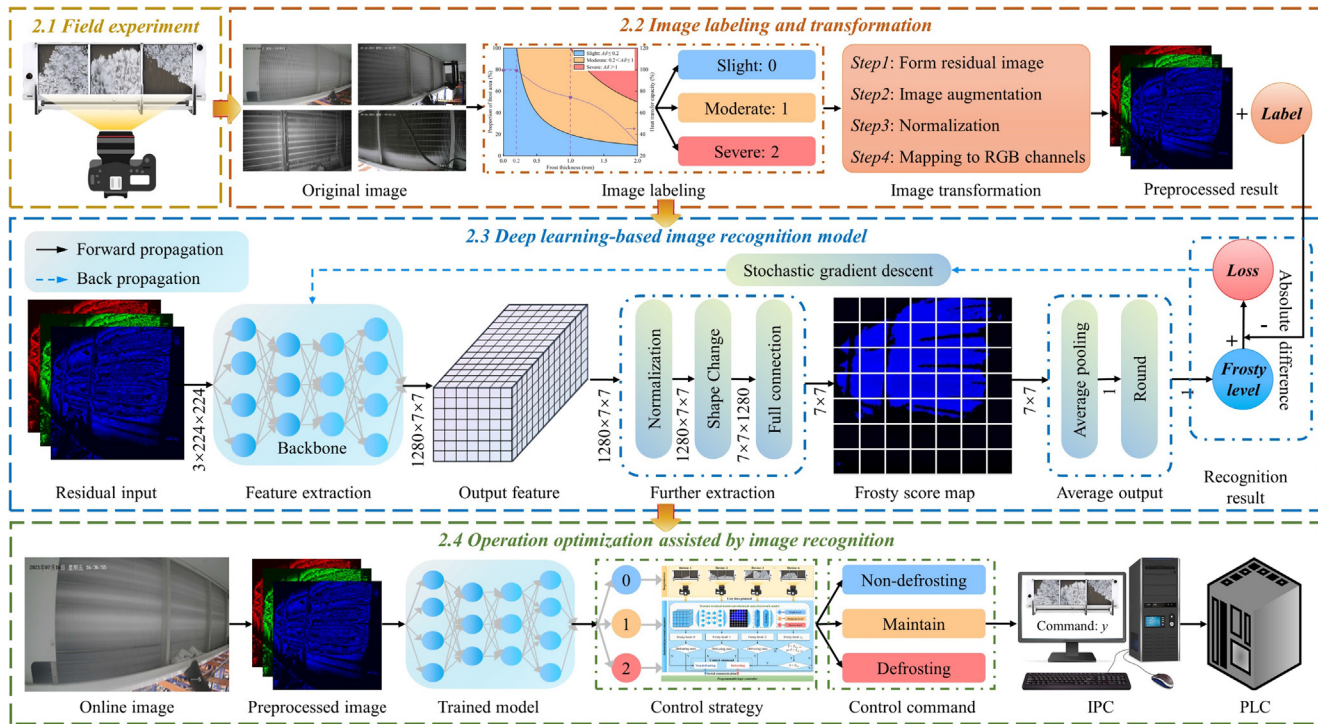


Fig. 1. Schematic overview of the proposed defrosting control optimization method.

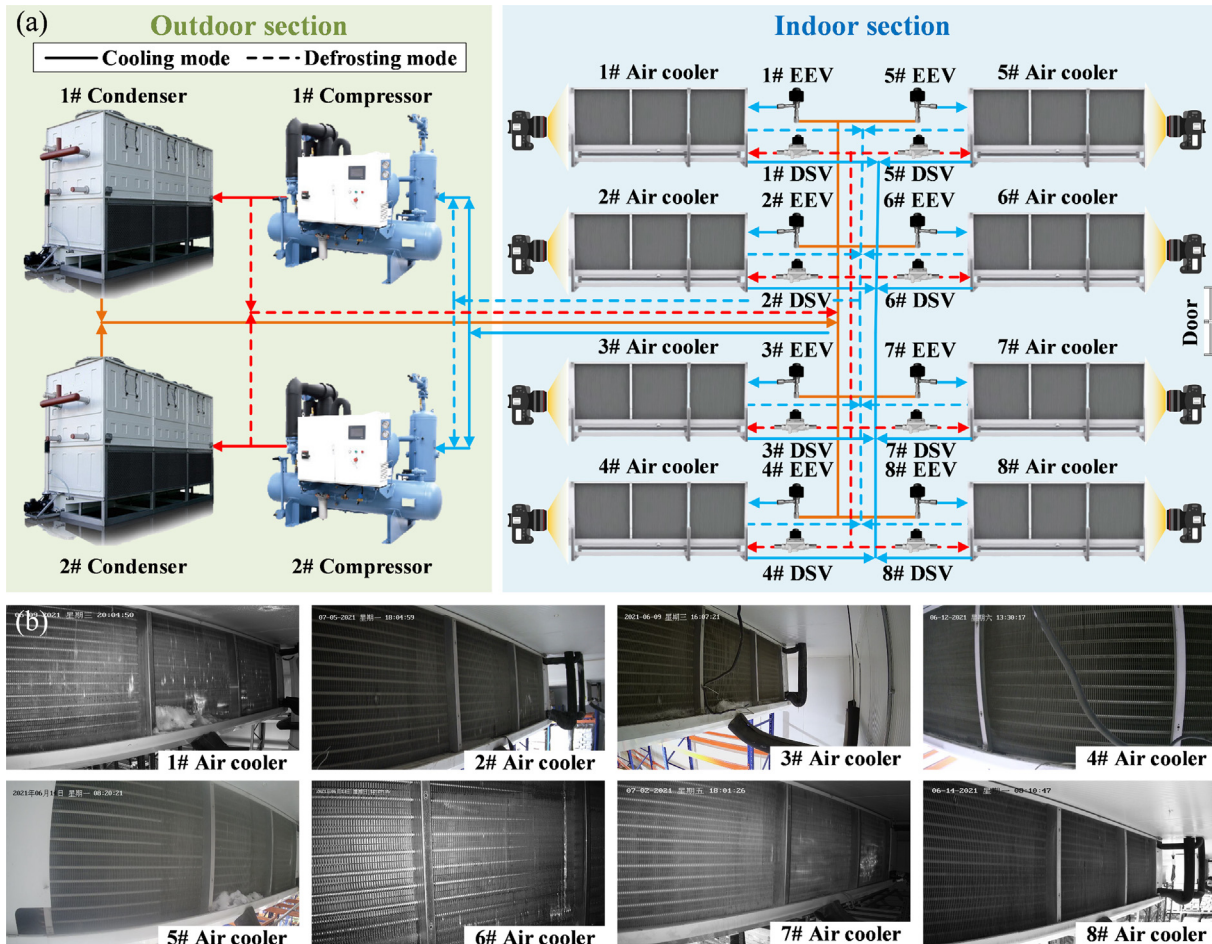


Fig. 2. Field experiments of refrigeration system in a cold storage. (a) Schematic diagram of the experiment setup. (b) Shooting angle and illuminance intensity of each air cooler.

Operation optimization assisted by image recognition

We move on to apply the deep learning-based image recognition model introduced in the previous section to optimize the operation control for industrial energy systems, i.e., defrosting optimization control. Depending on the real-time recognition of frosty level, a novel defrosting optimization control strategy is presented to initiate and terminate the defrosting operation on demand instead of on time or only initiating on demand. The flowchart of optimized defrosting control strategy assisted by image recognition is shown in Fig. 3, which is developed by four criteria: (1) The defrosting instruction is initiated when the frosty state reaches the severe level and terminated until it returns to the slight level; (2) With the principle of proper operation of HVAC systems, the defrosting instruction will not be implemented when the indoor temperature (T) is higher than the preset value ($T_{up, set}$) in cooling mode or lower than the preset value ($T_{low, set}$) in heating mode; (3) In order to maintain the indoor temperature, the number of devices in defrosting mode (N) is supposed to be less than the preset value (N_{set}) at the same time; (4) When N is larger than N_{set} , the excess will be put into the waiting queue and sequentially execute the defrosting command according to the waiting time. In this study, $T_{up, set}$ and N_{set} are -18°C and 2, respectively. Based on the current frosty level and above-mentioned defrosting control criteria, the IPC sends defrosting control commands to PLC via serial communication, and thus accomplishes the entire defrosting control process.

Results and discussion

Field experiment and image preprocessing

In the field experiment, 69,120 images were obtained by shooting each air cooler every 5 min, which are used for validating the presented method. By removing similar images with little variation in the frosty state, 20,393 images were retained for subsequent

preprocessing. Based on the proposed categorization criteria shown in Note S2 (online), the retained images were classified into three levels by manual labeling. The sample numbers of slight, moderate and severe levels are 10159, 4356 and 5878 respectively. Then, the labeled images were divided into the training dataset and testing dataset. Specifically, in order to train the RCNN model and test its recognition performance for trained air coolers, the images of 1–6# air coolers were divided into the training dataset and the testing dataset A in the proportion of 7:3. Meanwhile, all the images of the non-trained air coolers, 7# and 8#, were taken as the testing datasets B and C respectively for generalization performance validation. The sample numbers of each air cooler in four types of datasets are shown in Fig. 4a-d. The detailed description of four types of datasets is shown in Note S5 (online). After being manipulated by image transformation, the processed images were outputted to the RCNN model for model building and performance evaluation. Fig. 4e shows the complete image transformation process from the original image to the prepared input for the RCNN model.

Image recognition performance and generalization validation

Based on the images after the labeling and transformation mentioned above, the RCNN model is then trained and tested. Actually, the selection of the network backbone, learning rate, batch size and optimizer exerts direct influences on the recognition ability of the RCNN model. In order to obtain a better recognition performance, thirteen hyperparameter configurations are specially designed for hyperparameter optimization. The average accuracy of testing datasets A, B and C is used as the evaluating indicator for recognition performance comparison. The training and testing processes were conducted on a workstation equipped with the Intel Core i9-10900K central processor, Nvidia GeForce RTX 3080 graphics processor, 32-GB random access memory and 512-GB solid state disk. The comparison results verify the backbone of EfficientNet b0 (pre-trained on the ImageNet), the learning rate of

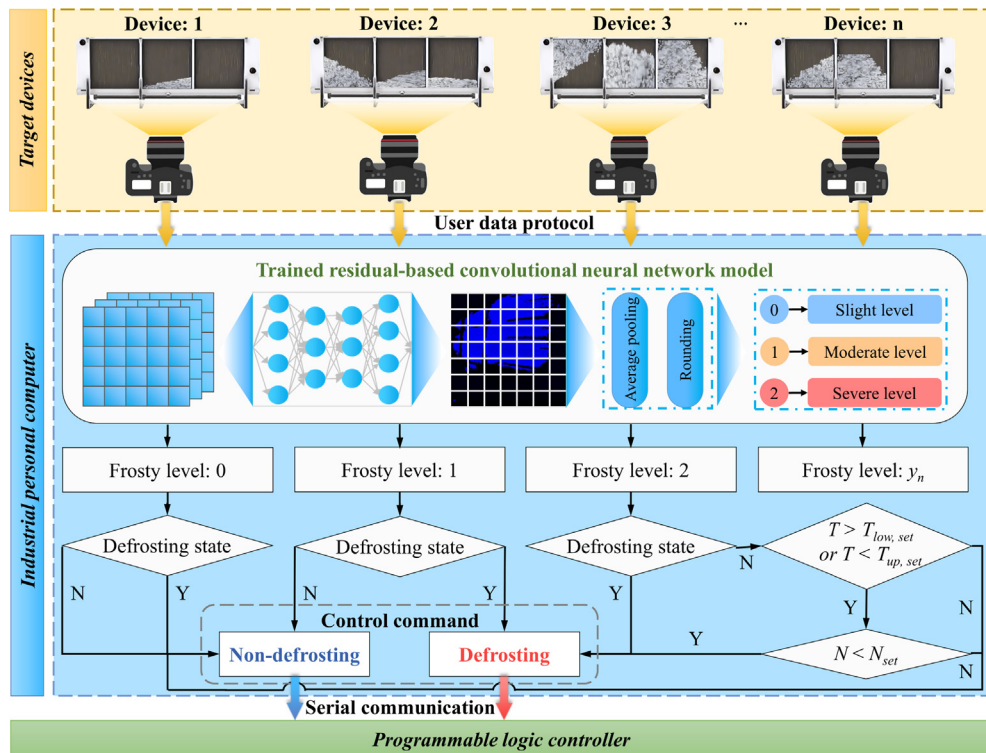


Fig. 3. Flowchart of optimized defrosting control strategy assisted by image recognition.

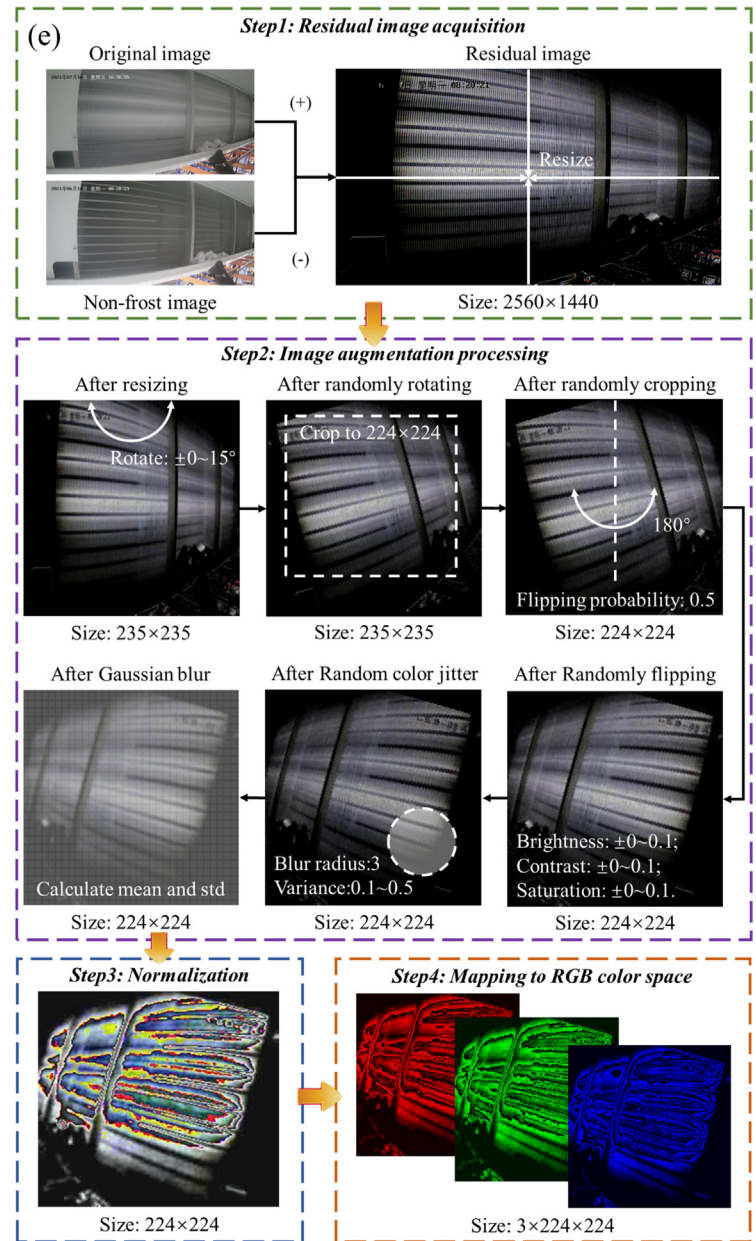
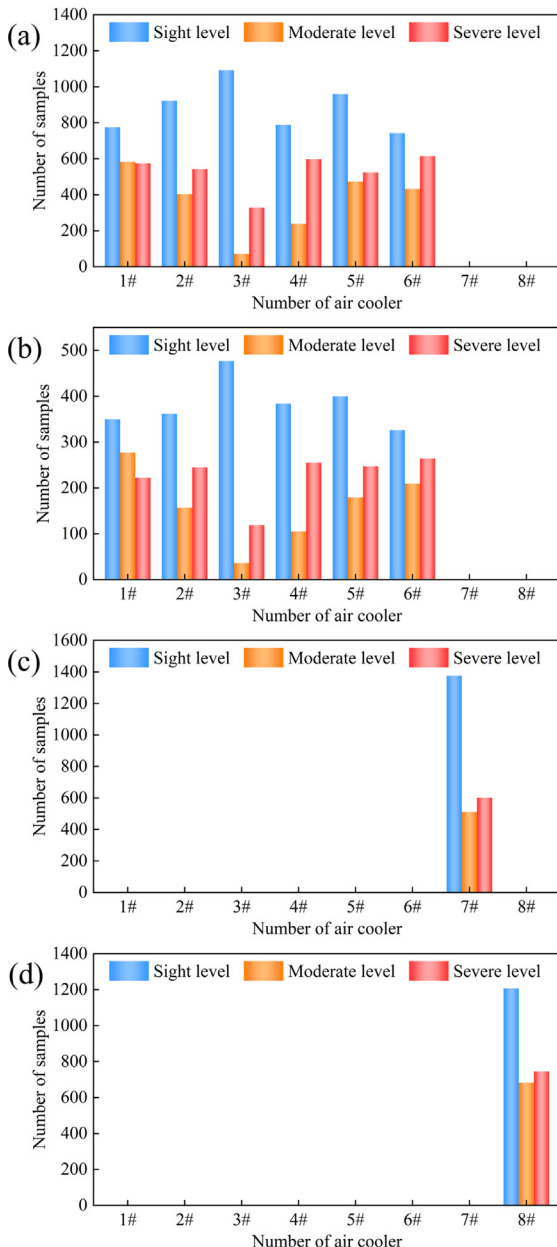


Fig. 4. Image transformation and labeling. (a-d) Sample numbers of each air cooler in (a) training dataset, (b) testing dataset A, (c) testing dataset B and (d) testing dataset C. (e) An example of image transformation process.

1×10^{-4} , the batch size of 4 and the optimizer of Adam are the optimal hyperparameter selection for the recognition task in this study. The detailed process of hyperparameter optimization was shown in Note. S6 (online).

Through the hyperparameter optimization process, the RCNN model was trained and tested under the selected optimal hyperparameter configuration. The RCNN model was trained for 20 epochs and the learning checkpoint was set to 500. The results of training and testing are shown in Fig. 5. As shown in Fig. 5a and 5b, the RCNN model was constantly learning the recognition task as the iteration increased, which was manifested in the continuous decline of the training loss and rise of the recognition accuracy in the training dataset. In Fig. 5c, the accuracy of testing dataset A rapidly reached 95% while that of testing datasets B and C slightly fluctuated near 90%. The average testing accuracy in Fig. 5d peaked at 94.13% in the 21000th iteration. After 21000 iterations, the training loss decreased to 0.255 and the training dataset accuracy increased to 95.74%. Meanwhile, the accuracies of testing datasets A, B and C respectively

attained 95.06%, 91.20% and 96.13%, i.e., the average recognition accuracy of 93.67% was obtained for non-trained 7# and 8# air coolers, which indicated that the RCNN model was well learned from the training dataset and maintained the strong generalization ability for non-trained air coolers in this learning process.

Fig. 5e-h shows the confusion matrices of frosty level recognition results using the RCNN model. The horizontal axis and vertical axis respectively represent the true frosty level and the classified frosty level. The results indicated that most of the images were correctly identified as their real labels no matter for trained air coolers or non-trained air coolers. In addition, although some images were classified into the wrong levels, the misclassifications mainly occurred between two adjacent frosting level instead of between slight level and severe level, which can avoid the severe faults in defrosting control. Therefore, the trained RCNN model was validated to combine high recognition reliability with excellent generalization performance, enabling the online application of defrosting optimization control method.

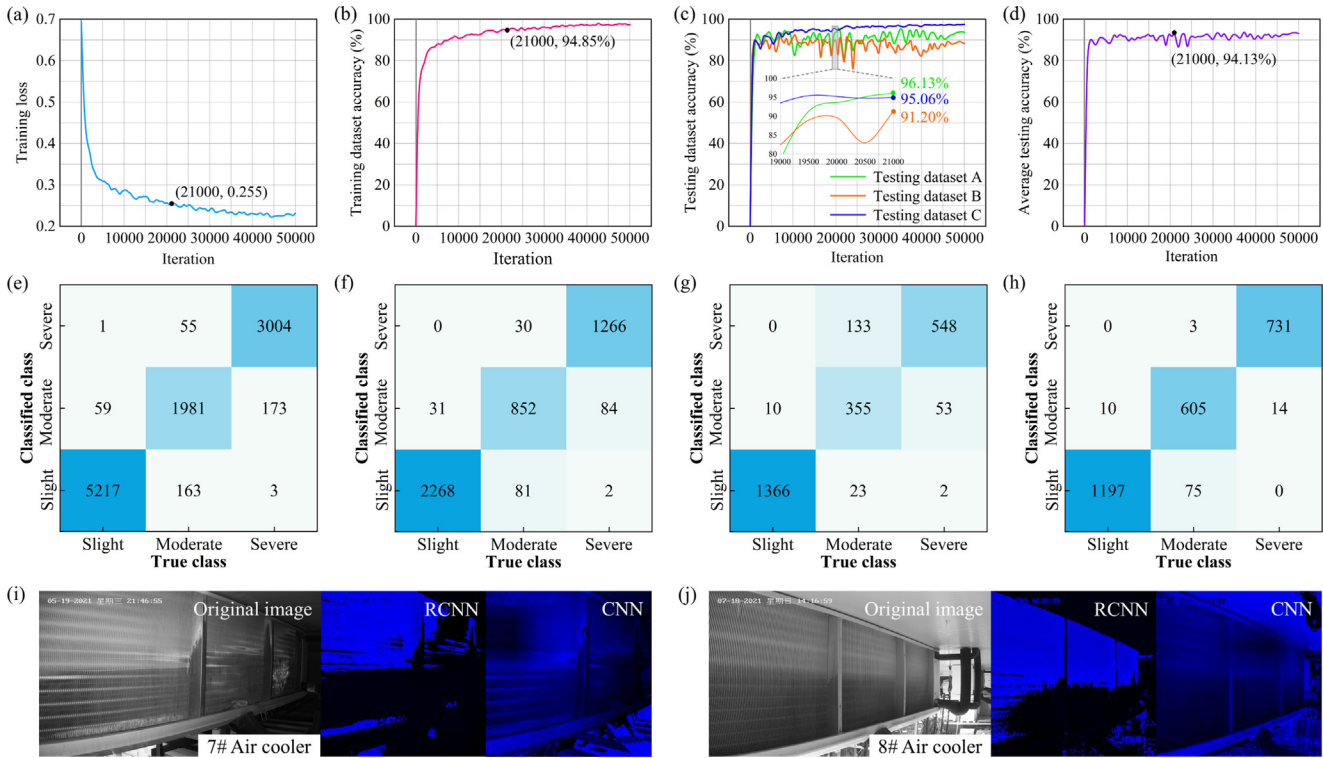


Fig. 5. Recognition performance and generalization ability of RCNN model. (a) Training loss. (b) Training dataset accuracy. (c) Testing dataset accuracy. (d) Average testing accuracy. (e-h) Confusion matrices of recognition results for (e) training dataset, (f) testing dataset A, (g) testing dataset B and (h) testing dataset C. (i-j) Comparison of feature extraction ability between RCNN and CNN for (i) 7# air cooler and (j) 8# air cooler.

Compared with the RCNN model, the input of the conventional CNN model was set as the original image and the output was obtained by the full connection. The conventional CNN was trained and tested under the same hyperparameter configuration as the RCNN model. The result of training and testing indicated that the accuracy of testing dataset A still exceeded 95% while that of testing datasets B and C dramatically fluctuated in a low level. Especially for the testing datasets B (7# air cooler), the recognition accuracies of slight, moderate and severe levels were respectively only 49.85%, 66.54% and 48.42%, which implied that the conventional CNN model failed to be directly applied in practical industrial systems due to the lack of generalization. The detailed training and testing results of conventional CNN model are shown in Note S7 (online). In order to further compare the feature extraction ability between the RCNN model and the conventional CNN model, the score map was converted to the score images through the bilinear up-sampling, which is shown in Fig. 5i-j. For the conventional CNN model, some irrelevant background objects such as frameworks and sidewalls were taken as the classification features, which led to the low generalization ability for non-trained objects. The detailed comparison of the feature extraction ability is shown in Note S8 (online).

Evaluation of optimized control

The optimal defrosting control strategy based on the RCNN model is further evaluated and analyzed in this section. The defrosting frequency, accumulated time and energy consumption of each air cooler were counted under the original control and the optimized control respectively, which is shown in Fig. 6a-c. With the application of defrosting optimization control strategy, the above-mentioned indicators of each air cooler experienced a sharp decline except 6# air cooler, which might be caused by the more severe and frequent frosting formation on the surface due

to the nearest distance to the door of cold storage. In general, the average defrosting frequency, accumulated time and energy consumption were respectively decreased from 46 to 21.25 times, from 1375.78 to 591.37 min and from 785 to 514.14 kW·h. The decline rate of defrosting frequency, accumulated time and energy consumption were respectively 53.8%, 57.02% and 34.5%. The results indicated that the proposed defrosting optimization control method could provide an effective way to decrease the switching frequency and energy consumption in the defrosting process for industrial energy systems.

In addition, the original time-based defrosting method may lead to the overtemperature operation in the cold storage. As illustrated in Fig. 6d, the indoor temperature is higher than the preset upper temperature for five days in the former month of the field experiment, which might pose growing risks of food spoilage and microbial growth. During this period, the refrigeration system operated in the normal temperature and pressure range without faults and power failures. The relative humidity was a bit higher in the range of 80% to 95%, so the surfaces of many air coolers were frosted severely. Due to the thick frost on the surfaces, the heat transfer coefficients and cooling capacity of air coolers decreased sharply, and thus causing the cold storage overtemperature. On the contrary, the overtemperature operation never happened after adopting the proposed defrosting control method. Therefore, the presented strategy also contributes to the stable operation of the refrigeration system.

The environmental and cost analysis is essential to evaluate the application potential and commercial value of the proposed method. The initial investment includes the purchase of surveillance cameras, the hardware upgrade of IPC and labor costs for equipment installation and image labeling. The total cost is approximately \$320. The guaranteed service life is at least 5 years. The estimation of reduction in CO₂ emissions [30] is shown in Fig. 6e. Within the guaranteed lifetime, the annual decreased CO₂

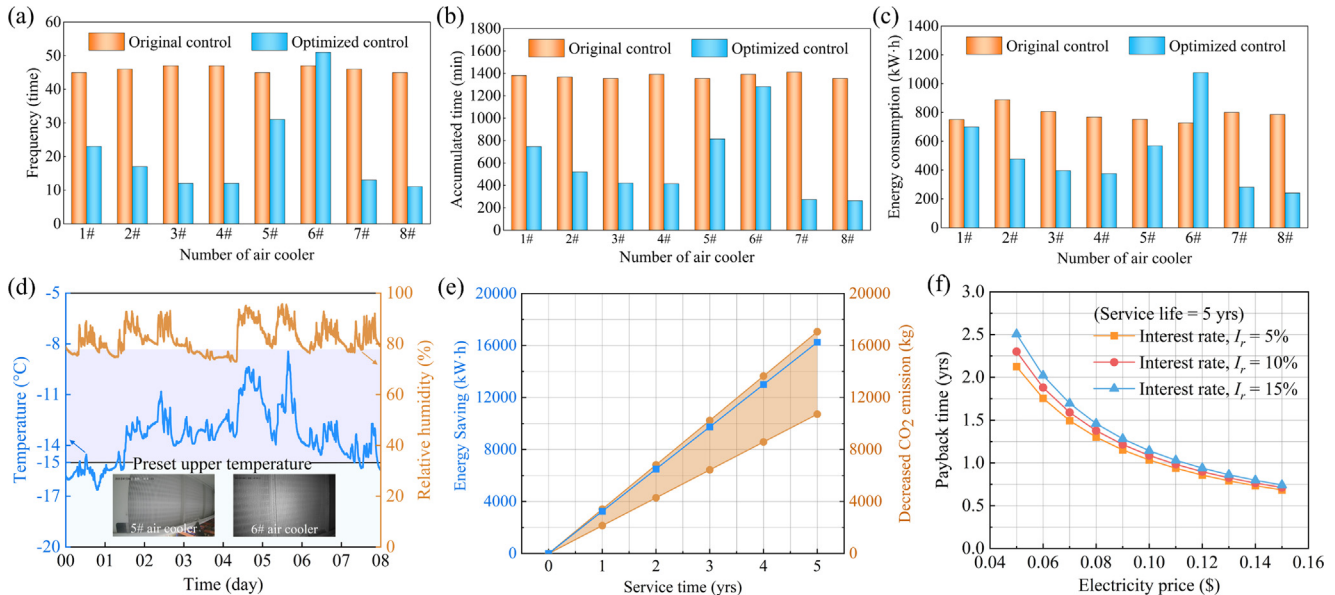


Fig. 6. Evaluation of optimized control. (a-c) Comparison of defrosting (a) frequency, (b) accumulated time and (c) energy consumption between original control and optimized control. (d) Example of cold storage overtemperature caused by original control. (e) Estimation of decreased CO₂ emissions for optimized control. (f) Estimation of payback years for optimized control.

emissions is approximately 2145.21 to 3412.84 kg. The electricity price varies from \$0.05 to \$0.15 based on the peak-valley pricing policy in Nanjing. The estimation of payback years [31] in different annual interest rates (5%, 10% or 15%) are shown in Fig. 6f. The maximum payback time is 2.5 years while the interest rate and electricity price are 15% and \$0.05 respectively, which is far below the service life. The detailed estimation process is shown in Note. S9 (online). The results of environmental and cost analysis indicate that proposed method provides an eco-friendly and energy-saving technology with highly commercial development value for energy enterprises.

Furthermore, there is still plenty of room to improve the technical feasibility of the proposed image recognition-based control optimization method. Firstly, the pre-trained model is supposed to be specifically designed according to the specific recognition task. The utilization of pre-trained model enhances the training speed and the accuracy of image recognition model, which is shown in Note. S10 (online). For the rapid extension in homotypic or heterotypic energy systems, the representative images need to be collected from lots of devices to train the initialized image recognition model before fine tuning in the specific devices. Secondly, the image recognition method is supposed to be upgraded to object detection from only image classification. In order to decrease the initial investment, the operation states of multiple devices would be shot by one surveillance camera in practical application, and thus the object detection model is necessary to be applied for the image recognition of multiple devices at the same time. Thirdly, the image recognition-based control strategy is supposed to integrate necessary expert rules to improve the operation reliability in practical energy systems. The above measures will further promote the commercial application of image recognition technology in industrial energy systems for energy saving and emission reduction.

Conclusion

In summary, we presented a novel deep learning-based image recognition method to assist energy saving and emission reduction for a typical industrial energy system and prove its technical feasibility through the field experiment. The main conclusions are obtained as follows:

- (1) By integrating the domain knowledge and advanced image recognition technique, the proposed RCNN model enables both high recognition accuracy and strong generalization ability. The recognition accuracy of RCNN model was 95.06% for the trained objects and 93.67% for non-trained objects while that of only 75.86% for the conventional CNN model.
- (2) According to the real-time image recognition for frosty levels, a novel defrosting control optimization method was presented to initiate and terminate the defrosting operation on demand. By adopting the presented control method, the defrosting frequency, accumulated time and energy consumption were 53.8%, 57.02% and 34.5% less than the original control method.
- (3) The environmental and cost analysis were conducted to determine the application potential and commercial value of the proposed method. The analysis results illustrated that the annual reduction in CO₂ emissions is approximately 2145.21 to 3412.84 kg and the payback time was less than 2.5 years which was far below the service life.

Therefore, the proposed RCNN model provides a powerful tool for the high-accuracy and high-generalization implementation of image recognition in industrial scenarios by integrating well-designed deep learning model with specific energy domain knowledge. By adopting the proposed image recognition-based control optimization method, the energy consumption is significantly reduced through the field test in the real industrial energy system, which shows strong potential for commercial application. Furthermore, frost formation is one of the most detrimental and common problems that happen on the heat exchangers in energy systems. Our method combining the specifically designed deep learning model with energy domain knowledge can be easily extended to efficiently optimize other industrial energy systems such as heat pumps, freezers and fresh air systems, illustrating the power of deep learning methods to accelerate the pace of carbon neutrality in industrial energy systems. Our study will shed light on the commercial application of image recognition technology for energy saving and emission reduction in industrial energy systems.

Declaration of Competing Interest

The authors declare that they have no known competing financial interests or personal relationships that could have appeared to influence the work reported in this paper.

Acknowledgements

This work was supported by the National Natural Science Foundation of China (No. 51876119) and the National Key R&D Program of China (2021YFE0107400).

Compliance with ethics requirements

This article does not contain any studies with human or animal subjects.

Appendix A. Supplementary material

Supplementary data to this article can be found online at <https://doi.org/10.1016/j.jare.2022.07.003>.

References

- [1] Aboudi J, Vafaeenezadeh M. Efficient and reversible CO₂ capture by amine functionalized-silica gel confined task-specific ionic liquid system. *J Adv Res* 2015;6(4):571–7.
- [2] Zhang W, Zhou T. Increasing impacts from extreme precipitation on population over China with global warming. *Sci Bull* 2020;65(3):243–52.
- [3] Hady AA. Deep solar minimum and global climate changes. *J Adv Res* 2013;4(3):209–14.
- [4] Li Q. The view of technological innovation in coal industry under the vision of carbon neutralization. *Int J Coal Sci Technol* 2021;8(6):1197–207.
- [5] Abdelaziz EA, Saidur R, Mekhilef S. A review on energy saving strategies in industrial sector. *Renew Sustain Energy Rev* 2011;15(1):150–68.
- [6] Bayoumy SH, El-Marsafy SM, Ahmed TS. Optimization of a saturated gas plant: meticulous simulation-based optimization – a case study. *J Adv Res* 2020;22:21–33.
- [7] Cui Y, Geng Z, Zhu Q, Han Y. Review: multi-objective optimization methods and application in energy saving. *Energy* 2017;125:681–704.
- [8] Zhu Xu, Chen K, Anduv B, Jin X, Du Z. Transfer learning based methodology for migration and application of fault detection and diagnosis between building chillers for improving energy efficiency. *Build Environ* 2021;200:107957. doi: <https://doi.org/10.1016/j.buildenv.2021.107957>.
- [9] LeCun Y, Bengio Y, Hinton G. Deep learning. *Nature* 2015;521(7553):436–44.
- [10] Nolazco-Flores JA, Faundez-Zanuy M, Velázquez-Flores OA, Del-Valle-Soto C, Cordasco G, Esposito A. Mood state detection in handwritten tasks using PCA-mFCBF and automated machine learning. *Sensors* 2022;22(4):1686. doi: <https://doi.org/10.3390/s22041686>.
- [11] Narciso DAC, Martins FG. Application of machine learning tools for energy efficiency in industry: a review. *Energy Rep* 2020;6:1181–99.
- [12] Xu Y, Yan C, Liu H, Wang J, Yang Z, Jiang Y. Smart energy systems: a critical review on design and operation optimization. *Sustain Cit Soc* 2020;62:102369. doi: <https://doi.org/10.1016/j.scs.2020.102369>.
- [13] Zhao Y, Zhang C, Zhang Y, Wang Z, Li J. A review of data mining technologies in building energy systems: load prediction, pattern identification, fault detection and diagnosis. *Energy Built Environ* 2020;1(2):149–64.
- [14] Vakiloroaya V, Samali B, Fakhar A, Pishghadam K. A review of different strategies for HVAC energy saving. *Energy Convers Manage* 2014;77:738–54.
- [15] Zhang X, Liu C, Shen C, Liu X. Promising commercial fabrics with radiative cooling for personal thermal management. *Sci Bull* 2022;67(3):229–31.
- [16] Han B, Xiong T, Xu S, Liu G, Yan G. Parametric study of a room air conditioner during defrosting cycle based on a modified defrosting model. *Energy* 2022;238:121658. doi: <https://doi.org/10.1016/j.energy.2021.121658>.
- [17] Buick TR, McMullan JT, Morgan R, Murray RB. Ice detection in heat pumps and coolers. *Int J Energy Res* 1978;2(1):85–98.
- [18] Ge Y, Sun Y, Wang W, Zhu J, Li L, Liu J. Field test study of a novel defrosting control method for air-source heat pumps by applying tube encircled photoelectric sensors. *Int J Refrig* 2016;66:133–44.
- [19] Matsumoto K, Koshizuka M, Honda M, Tsubaki D, Murase M, Furudate Y. Measurement on nano scale by scanning probe microscope for obtaining real ice adhesion force. *Int J Refrig* 2014;41:181–9.
- [20] Muller E. A new concept for defrosting refrigeration plants. *Kalte*. 1975;28:52–4.
- [21] Payne V, O'Neal DL. Defrost cycle performance for an air-source heat pump with a scroll and a reciprocating compressor. *Int J Refrig* 1995;18(2):107–12.
- [22] Qu K, Komori S, Jiang Yi. Local variation of frost layer thickness and morphology. *Int J Therm Sci* 2006;45(2):116–23.
- [23] Song M, Dang C. Review on the measurement and calculation of frost characteristics. *Int J Heat Mass Transf* 2018;124:586–614.
- [24] Li Z, Wang W, Sun Y, Wang S, Deng S, Lin Y. Applying image recognition to frost built-up detection in air source heat pumps. *Energy* 2021;233:121004. doi: <https://doi.org/10.1016/j.energy.2021.121004>.
- [25] Xu Bo, Han Q, Chen J, Li F, Wang N, Li D, et al. Experimental investigation of frost and defrost performance of microchannel heat exchangers for heat pump systems. *Appl Energy* 2013;103:180–8.
- [26] Zheng X, Shi R, You S, Han Y, Shi K. Experimental study of defrosting control method based on image processing technology for air source heat pumps. *Sustain Cities Soc* 2019;51:101667. doi: <https://doi.org/10.1016/j.scs.2019.101667>.
- [27] Tan M, Le Q. Efficientnet: Rethinking model scaling for convolutional neural networks. *Int Conf Mach Learn*. 2019;6105–14.
- [28] Hu J, Shen L, Sun G. Squeeze-and-excitation networks. In: Proceedings of the IEEE Conference on Computer Vision and Pattern Recognition. p. 7132–41.
- [29] Xie S, Girshick R, Dollár P, Tu Z, He K. Aggregated Residual Transformations for Deep Neural Networks. In: Proceedings of the IEEE Conference on Computer Vision and Pattern Recognition. p. 5987–95.
- [30] Wang M, Yao M, Wang S, Qian H, Zhang P, Wang Y, et al. Study of the emissions and spatial distributions of various power-generation technologies in China. *J Environ Manage* 2021;278:111401. doi: <https://doi.org/10.1016/j.jenvman.2020.111401>.
- [31] Bait O. Exergy, environ-economic and economic analyses of a tubular solar water heater assisted solar still. *J Cleaner Prod* 2019;212:630–46.